

Proceedings of the Seventh World Conference on Earthquake Engineering

VOLUME 3

Geotechnical Aspects



September 8-13, 1980

PROCEEDINGS OF THE 10191 86.218
SEVENTH WORLD
CONFERENCE ON
EARTHQUAKE ENGINEERING
E 115
V. 3

September 8-13, 1980
Istanbul, Turkey



7th WCEE
ISTANBUL 1980

VOLUME

3

GEOTECHNICAL ASPECTS

DYNAMIC PROPERTIES AND BEHAVIOUR
OF SOILS AND ROCKS

DYNAMIC PROPERTIES AND BEHAVIOUR
OF SOIL AND ROCK STRUCTURES

GEOTECHNICAL EXPERIMENTAL INVESTIGATIONS

DYNAMIC PROPERTIES AND BEHAVIOUR OF
FOUNDATIONS, PILES AND RETAINING WALLS

TABLE OF CONTENTS

FIELD AND CONSTITUTIVE EQUATIONS FOR A TWO-PHASE MEDIUM FOR ANALYSIS OF THE BEHAVIOR OF IN-SITU SOIL DEPOSITS	1
Jean H. Prevost	
A FINITE DIFFERENCE MODEL FOR LIQUEFACTION ANALYSIS	9
Atilla M. Ansal, Ali A. Elzaroughi, Raymond J. Krizek, Zdenek P. Bazant	
SOIL PARAMETERS AFFECTING PORE-PRESSURE BUILDUP DURING EARTHQUAKES	17
Mehmet A. Sherif, Isao Ishibashi, Wen-Lon Cheng	
LIQUEFACTION POTENTIAL OF SATURATED SAND: THE STIFFNESS METHOD	25
R. Dobry, D.J. Powell, F.Y. Yokel, R.S. Ladd	
GROUND CONDITION AND DISASTER OF THE 1978 MIYAGI-KEN-OKI EARTHQUAKE IN JAPAN.....	33
Tsuneo Imai, Takeshi Okubo,	
ANALYSIS OF A DEVICE FOR IN-SITU MEASUREMENT OF THE SHEAR MODULUS OF SOIL AT LARGE STRAINS	41
Joaguin Marti, Luis Rodriguez-Ovejero	
NATURAL SLOPE FAILURES DURING EARTHQUAKES: A CASE STUDY	49
S. Okusa, F. Tatsuoka, E. Taniguchi, Y. Ohkochi	
DYNAMIC SHEAR MODULUS AND DAMPING IN ADDITIVE: TREATED EXPANSIVE SOILS	57
Yong S. Chae, Wing-cheong Au	
DYNAMIC PROPERTIES OF FROZEN SAND UNDER SIMULATED EARTHQUAKE LOADING CONDITIONS	65
Ted. S. Vinson, John C. Li	
EFFECTIVE STRESS METHOD IN ONE-DIMENSIONAL SOIL RESPONSE ANALYSIS	73
Kenji Ishihara, Ikuo Towhata	
A DEVICE FOR THE IN-SITU MEASUREMENT OF THE DYNAMIC MODULI OF SOILS AT LARGE STRAINS	81
Roger C.H. Sidey, Richard H. Bassett	
LIQUEFACTION OF MINE TAILINGS IN THE 1978 IZU-OHSHIMA-KINKAI EARTHQUAKE, CENTRAL JAPAN	89
Shigeyasu Okusa, So Anna, Hiromu Maikuma	
PROBABILITY OF LIQUEFACTION DUE TO EARTHQUAKE	97
I-Hsin Chou, J.L. Ehasz	
METHODS FOR THE PREDICTION OF SAND LIQUEFACTION	105
Liu Ying	
EXPERIMENTAL DETERMINATION OF DYNAMIC PASSIVE PRESSURE OF SAND	113
P. Nandakumaran, V.S. Prasad	

EVALUATION OF LIQUEFACTION STRENGTH OF SANDY SOILS	121
Koichiro Yokota	
LIQUEFACTION ANALYSIS OF HORIZONTALLY LAYERED SAND CONSIDERING A Laterally Confined Condition	125
Fusao Oka, Kouzi Sekiguchi	
SEISMIC ANALYSIS OF EARTH SLOPES: A CASE STUDY	129
Dimitri Athanasiou-Grivas, Gregory F. Nadeau	
MICROSTRUCTURAL EFFECTS ON DYNAMIC RESPONSE OF CLAYS	133
Tuncer B. Edil, Gwo-Fea Luh	
SEISMIC RESPONSE OF THE GROUND AND EARTHQUAKE DAMAGE IN NAGOYA AREA, JAPAN	141
Kazuaki Masaki, Kumizi Lida	
ENDOCHRONIC THEORY OF SAND LIQUEFACTION	149
W.D. Liam Finn, Shobha Bhatia	
EVALUATION OF THE LIQUEFACTION OF SAND BY STATIC CONE PENETRATION TEST	156
Zhou Shengen	
EFFECT ON ANISOTROPIC CONSOLIDATION ON LIQUEFACTION	163
Ali Erguvanli	
EARTHQUAKE DAMAGE OF BAIHE EARTH DAM AND LIQUEFACTION CHARACTERISTICS OF SAND AND GRAVEL MATERIALS	171
Liu Lingyao, Li Kueifen, Bing Dangping	
ANALYSIS OF SOIL LIQUEFACTION DURING 1979 MONTENEGRO EARTHQUAKE	179
Kosta Talaganov, Vladimir Mihailov, Trajko Bogoevski	
THE INFLUENCE OF SEISMIC LOADING ON THE BEHAVIOUR OF TWO ISTANBUL CLAYS	187
E. Togrol, A. Sağlamer, K. Özudogru, E. Güler	
STUDIES ON SOIL LIQUEFACTION OBSERVED DURING THE MIYAGI-KEN OKI EARTHQUAKE OF JUNE 12, 1978	195
Toshio Iwasaki, Ken-ichi Tokida	
THE LIQUEFACTION SUSCEPTIBILITY OF SOME GREEK SEISMIC AREAS AND THE FACTOR WHICH CONTROL IT	203
K. Andrikopoulou, A. Roussopoulos	
ANALYSIS OF LIQUEFACTIONS DURING THE 1978 OFF MIYAGI PREFECTURE EARTHQUAKE	211
Hajime Tsuchida, Susumu Iai, Satoshi Hayashi	
GEOLOGICAL AND SOIL MECHANICAL STUDIES ON DAMAGE TO HOUSING SITES BY THE MIYAGI-KEN-OKI EARTHQUAKE, 1978	219
A. Asada, F. Kawakami, E. Yanagisawa	

FORMULAE FOR PREDICTING LIQUEFACTION POTENTIAL OF CLAYEY SILT AS DERIVED FROM A STATISTICAL METHOD	227
Wang Yuding, Luan Fang, Han Qingyu, Li Guoxin	
LIMIT ANALYSIS OF SEISMIC SLOPE STABILITY	235
S.W.Chan, W.F. Chen, S.L. Koh	
BEARING CAPACITY UNDER SEISMIC LOADING	242
Surendra K. Saxena	
THE ANALYSIS OF LIQUEFACTION POTENTIAL BASED ON PROBABILISTIC GROUND MOTIONS	249
Milton A. Deherrera, Theodore C. Zautty	
LIQUEFACTION TEST UNDER A PARTIAL DRAINAGE CONDITION AND ITS APPLICATION	253
Yasufumi Umehara, Kouki Zen, Kouji Hamada	
INSITU MEASUREMENT OF DYNAMIC CHARACTERISTICS ON AN EARTH DAM	257
Satyendra P. Gupta, L.S. Srivastava, P. Nandakumaran, S. Mukerjee	
A STIFFNESS MATRIX APPROACH FOR LAYERED SOILS	265
E. Kausel, J. M. Roesset, G. Bouckoválas	
SPATIAL VIBRATION STUDY OF AN EARTH DAM	273
G.S. Seleznyev, Kh, Sh. Abduraufov	
CYCLIC UNDRAINED STRENGTH OF SAND BY TRIAXIAL TEST AND SIMPLE SHEAR TEST	281
Marshall L. Silver, Fumio Tatsuoka, Apichart Phukunhaphan, Anastis S. Avramidis.	
DETERMINING DYNAMIC DEFORMATION CHARACTERISTICS OF SOILS BY IN-SITU MEASUREMENTS AND LABORATORY TESTING	289
Tsuneo Imai, Keiji Tonouchi	
CROSSHOLE SURVEY AT A NUCLEAR POWER PLANT SITE	297
H. Turan Durgunoğlu, Semih S. Tezcan, Selçuk Erden, Yalçın Acar	
CYCLIC TRIAXIAL TEST OF DYNAMIC SOIL PROPERTIES FOR WIDE STRAIN RANGE	305
Takeji Kakusho	
EMPIRICAL PROCEDURE FOR PORE PRESSURE PREDICTION IN SANDS	313
M.K. Yegian	
A RE-EXAMINATION OF THE EFFECT OF PRIOR LOADINGS ON THE LIQUEFACTION OF SANDS	321
Sukhmander Sing, Neville C. Donovan, Ted K. Park	

THE GENERATION OF PORE PRESSURES IN CLAYEY SOILS DURING EARTHQUAKES	326
Kutay Özeydin, Ali Erguvanlı	
SEISMIC STABILITY CALCULATIONS OF EARTH AND ROCK FILL DAMS.....	331
N.D. Krasnikov, O.A. Savinov, A.P. Troitsky, V. I. Khorkov	
PRELIMINARY ANALYSIS OF DAMAGE TO THE BAI RIVER AND THE CHIAO RIVER DAM	339
Zhang Kexu	
DYNAMIC PROPERTIES OF A WEATHERED ROCK	347
I.H.Wong, K.H.Liu, J.L. Ehasz	
INVESTIGATION OF CYCLIC STRESS-STRAIN CHARACTERISTICS OF GRAVEL MATERIAL	355
J.Studer, N. Zingg, E.G. Prater	
EXPERIMENTAL STUDY ON LIQUEFACTION OF SANDY SOIL ON COHESIVE LAYER	363
Yukitake Shioi	
AN INVESTIGATION INTO THE LIQUEFACTION POTENTIAL AND MEASURES TAKEN TO COUNTER UNDER REFINERY.....	367
R.K.M. Bhandari	
DYNAMIC PROPERTIES OF EARTH DAMS	371
Ahmed M. Abdel- Ghaffar, Ronald Scott	
INELASTIC DYNAMIC RESPONSE OF SATURATED SOILS	379
Chris A. Katsikas, E. Benjamin Wylie	
SOIL LIQUEFACTION EVALUATION WITH USE OF STANDARD PENETRATION RESISTANCES	387
Susumu Yasuda, Ken-ichi Tokida	
EFFECTS ON SITE RESPONSE OF METHODS OF ESTIMATING IN SITU. NONLINEAR SOIL BEHAVIOR	395
K.H. Stokoe, A.T.F.Chen	
EARTHQUAKE RESPONSE CHARACTERISTICS OF STRUCTURE WITH PILE FOUNDATION ON SOFT SUBSOIL LAYER AND ITS SIMULATION ANALYSIS	403
T.Ohta, S. Uchiyama, M. Niwa, K. Ueno	
ON CHARACTERISTICS OF EARTHQUAKE BEHAVIOR OF CAISSON-PIER	411
Masao Satake, Teruo Asano	
CONVENIENT ASEISMIC DESIGN OF PILE FOUNDATION	419
Yasuyuki Esashi, Yasuo Yoshida	
ANALYSIS OF PILES IN SAND AGAINST EARTHQUAKES	427
V. Chandrasekaran, Shamsher Prakash	

EARTHQUAKE OBSERVATION AND NUMERICAL ANALYSIS OF DYNAMIC STRAIN OF FOUNDATION PILE	435
Masanori Hamada, Osamu Ishida	
PARTICIPATION FACTOR OF HORIZONTAL FORCE APPLIED TO PILE FOUNDATION	443
Yoshihiro Sugimura	
ENGINEERING APPROACH TO MODELING OF FILED SYSTEMS	451
Rodrigo Flores Coombs, Manuel Americo G. Silva	
DYNAMIC AND STATIC TEST OF MODEL PILES OF PILE GROUPS	459
Shintaro Yao	
TRAVELLING WAVES IN A GROUP OF PILES TAKING PILE-SOIL-PILE INTERACTION INTO ACCOUNT	467
John P. Wolf, Guido A. Von Arx	
EARTHQUAKE RESPONSE OF TURBOMACHINERY FRAME FOUNDATIONS	471
M.Novak, F. Aboul-Ella	
DYNAMIC POISSON'S RATIO OF SOIL	475
Koichiro Yokota, Masashi Konno	
EFFECTS OF GROUND STRUCTURES WITH Laterally Steep Variations ON SEISMIC MOTIONS	479
Kojiro Irikura, Shigeru Kasuga	
SEISMICALLY INDUCED DEFORMATIONS IN EARTHDAMS	483
Ronald C. Chaney	

FIELD AND CONSTITUTIVE EQUATIONS FOR A TWO-PHASE MEDIUM FOR ANALYSIS OF THE BEHAVIOR OF IN-SITU SOIL DEPOSITS

Jean H. Prévost⁽¹⁾

SUMMARY

Field and constitutive equations for the treatment of soil as a two-phase medium in boundary value problems are presented. A number of examples which demonstrate the versatility and accuracy of the proposed formulation are shown.

INTRODUCTION

Soil consists of an assemblage of particles with different sizes and shapes which form a skeleton whose voids are filled with various fluids. In cases in which some flow of the pore fluids takes place, there is an interaction between the skeleton strains and the pore-fluid flow. The solution of these problems therefore requires that soil behavior be analyzed by incorporating the effects of the flow (transient or steady) of the pore-fluids through the voids, and thus requires that a multiphase continuum formulation be available for soils. Such a theory was first developed by Biot [2] for an elastic porous skeleton. However, it is observed experimentally that the stress-strain behavior of the soil skeleton is strongly anelastic. An extension of Biot's theory into the nonlinear anelastic range is therefore necessary in order to analyze the transient response of soil deposits. Such an extension [10] of Biot's formulation is adopted herein. In order to relate the changes in effective stresses carried by the soil skeleton to the skeleton rate of deformations, a general analytical model [9] which describes the nonlinear, anisotropic, elastoplastic, stress and strain dependent, stress-strain-strength properties of the soil skeleton when subjected to complicated three-dimensional, and in particular to cyclic loading paths [7], is used. The model's extreme versatility and accuracy are demonstrated by applying it to represent the behavior of both cohesive and cohesionless soils under both drained and undrained, monotonic and cyclic loading conditions. The use of the proposed formulation for solving boundary value problems is thereafter illustrated.

FIELD EQUATIONS

For a saturated soil consisting of a macroscopically perfect fluid and a piecewise-linear time-independent porous skeleton wherein both the pore-fluid and the solid grains are incompressible, the coupled field equations take the following forms [10],

$$\begin{aligned} \operatorname{div}[\bar{\sigma}^s + \sigma^s \operatorname{div} \underline{v}^s] - \operatorname{div}[(\bar{p}_w + p_w \operatorname{div} \underline{v}^s)\underline{1}] + \\ \operatorname{div}[\underline{D}:\underline{L}^s] + \rho_w \operatorname{div} \underline{v}^s (\underline{b} - \underline{a}^w) + \rho_b^s \underline{\dot{\sigma}}^s = \rho_s^s \underline{\dot{\sigma}}^s + \rho_a^w \underline{\dot{a}}^w \end{aligned} \quad (1)$$

$$- \operatorname{div}\left[\frac{n}{\rho_w} k^{ws} \cdot (\operatorname{grad} p_w - \rho_w \underline{b} + \rho_w \underline{a}^w)\right] + \operatorname{div} \underline{v}^s = 0 \quad (2)$$

in which

⁽¹⁾ Asst. Prof. Civil Eng., Princeton University, Princeton, New Jersey.

$$D_{abcd} = \frac{1}{2} [\sigma_{bd} \delta_{ac} - \sigma_{ad} \delta_{bc} - \sigma_{ac} \delta_{bd} - \sigma_{bc} \delta_{ad}] \quad (3)$$

is a tensor arising from geometric changes; $\underline{\underline{\sigma}} = \underline{\underline{\sigma}}^s - p_w \underline{\underline{1}}$ is the total stress tensor [33]; and the subscript s and w refer to the solid and fluid phases, respectively. In Eqs. 1 and 2, $\underline{\underline{\sigma}}^s$ = effective Cauchy stress tensor; p_w = pore-fluid pressure; $\underline{\underline{v}}^\alpha$ = velocity of α -phase; $\underline{\underline{a}}^\alpha$ = acceleration of α -phase; $\underline{\underline{d}}^\alpha$ and $\underline{\underline{w}}^\alpha$ = symmetric and skew-symmetric parts of the velocity gradient $\underline{\underline{L}}^\alpha$, respectively; $\underline{\underline{k}}^{ws}$ = permeability tensor; ρ_α = microscopic mass density of α -phase; n^w = porosity; $\rho^s = (1-n^w)\rho_s$; $\rho = \rho^s + n^w \rho_w$; $\underline{\underline{b}}$ = body force density per unit mass; and a superimposed dot indicates the material derivative following the motion of the solid skeleton. In Eq. 1, $\underline{\underline{\dot{\sigma}}}^s$ denotes the Jaumann derivative viz.

$$\underline{\underline{\dot{\sigma}}}^s = \underline{\underline{\dot{\sigma}}}^s + \underline{\underline{\sigma}}^s \underline{\underline{w}}^s - \underline{\underline{w}}^s \underline{\underline{\sigma}}^s \quad (4)$$

CONSTITUTIVE EQUATIONS

The constitutive equations for the solid skeleton are written in one of the following forms [4]:

$$\underline{\underline{C}} : \underline{\underline{d}}^s = \begin{cases} \underline{\underline{\dot{\sigma}}}^s & \text{small deformations} \\ \underline{\underline{\dot{\sigma}}}^s + \underline{\underline{\sigma}}^s \text{div } \underline{\underline{v}}^s & \text{finite deformations} \end{cases} \quad (5)$$

$\underline{\underline{C}}_{abcd}$ is an (objective) tensor valued function of, possibly, $\underline{\underline{\dot{\sigma}}}^s$ and the deformation gradients. Many nonlinear material models of interest can be put in the above form (e.g. all nonlinear elastic materials, and many elastoplastic materials). For soil media [9],

$$\underline{\underline{C}} = \underline{\underline{E}} - \frac{1}{H' + \underline{\underline{Q}} : \underline{\underline{E}} : \underline{\underline{P}}} (\underline{\underline{E}} : \underline{\underline{P}}) (\underline{\underline{Q}} : \underline{\underline{E}}) \quad (6)$$

in which H' is the plastic modulus; $\underline{\underline{P}}$ and $\underline{\underline{Q}}$ are dimensionless symmetric second-order tensors, normalized in such a way that $\underline{\underline{P}} : \underline{\underline{P}} = \underline{\underline{Q}} : \underline{\underline{Q}} = 1$ and such that $\underline{\underline{P}}$ gives the direction of plastic deformations and $\underline{\underline{Q}}$ the outer normal to the active yield surface; and $\underline{\underline{E}}$ is the fourth-order tensor of elastic moduli, assumed isotropic for the particular class of material models implemented. The plastic potential is selected such that, in agreement with experimental observations, the plastic deviatoric rate of deformation vector remains normal to the projection of the yield surface onto the deviatoric stress subspace, i.e.,

$$\underline{\underline{P}} - \frac{1}{3} (\text{trace } \underline{\underline{P}}) \underline{\underline{1}} = \underline{\underline{Q}} - \frac{1}{3} (\text{trace } \underline{\underline{Q}}) \underline{\underline{1}} = \underline{\underline{Q}}' \quad (7a)$$

$$\text{trace } \underline{P} = \text{trace } \underline{Q} + A \frac{\text{trace } \underline{Q}}{|\text{trace } \underline{Q}|} \{Q':Q'\}^k \quad (7b)$$

in which A is a material parameter which measures the departure from an associative flow rule. When $A=0$, $\underline{P}=\underline{Q}$ and consequently the \underline{C} tensor possesses the major symmetry. The yield function is selected of the following form [9]

$$f = \frac{3}{2} (\underline{s}^s - \underline{\alpha}) : (\underline{s}^s - \underline{\alpha}) + C^2 (p'^s - \beta)^2 - k^2 = 0 \quad (8)$$

where \underline{s}^s is the deviatoric stress tensor (i.e. $\underline{s}^s = \underline{\sigma}^s - p'^s \underline{1}$, $p'^s = \frac{1}{3} \text{trace } \underline{\sigma}^s$); $\underline{\alpha}$ and β are the coordinates of the center of the yield surface in the deviatoric stress space and along the hydrostatic stress axis, respectively; k is the size of the yield surface; and C is a material parameter called the yield surface axis ratio. In order to allow for the adjustment of the plastic hardening rule to any kind of experimental data, for example, data obtained from axial or simple shear soil tests, a collection of nested yield surfaces is used. A plastic modulus is associated with each of the yield surfaces, and

$$H' = h' + \frac{\text{trace } \underline{Q}}{(3Q:Q)^{\frac{1}{k}}} B' \quad (9)$$

where h' is the plastic shear modulus and $(h' + B')$ are the plastic bulk moduli associated with f which are mobilized in consolidation tests upon loading and unloading, respectively. The projections of the yield surfaces onto the deviatoric stress subspace thus define regions of constant plastic shear moduli. For a soil element whose anisotropy initially exhibits rotational symmetry about the y -axis, $\alpha_x = \alpha_z = -\alpha_y/2$ and Eq. 8 simplifies to

$$[(\sigma_y'^s - \sigma_x'^s) - \alpha]^2 + C^2 (p'^s - \beta)^2 - k^2 = 0 \quad (10)$$

in which $\alpha = 3\alpha_y/2$. The yield surfaces then plot as ellipses in the axisymmetric stress plane $(\sigma_x'^s = \sigma_z'^s)$ as shown in Fig. 1. Points C and E on the outer-most yield surface define the critical state conditions (i.e., $H'=0$) for axial compression and extension loading conditions, respectively [6]. It is assumed that the slopes of the critical state lines OC and OE remain constant during yielding.

The yield surfaces are allowed to change in size as well as to be translated by the stress point. Their associated plastic moduli are also allowed to vary in and, in general, both k and H' are functions of the plastic strain history. They are conveniently taken as functions of invariant measures of the amount of plastic volumetric strains and/or plastic shear distortions, respectively [7].

Complete specification of the model parameters requires the determination of (i) the initial positions and sizes of the yield surfaces together with their associated plastic moduli; (ii) their size and/or plastic modulus changes as loading proceeds, and finally, (iii) the elastic shear G and bulk B moduli. The soil's anisotropy originally develops during its

deposition and subsequent consolidation which, in most practical cases, occurs under no lateral deformations. In the following, the y-axis is vertical and coincides with the direction of consolidation, and the material's anisotropy initially exhibits rotational symmetry about the vertical y-axis. The model parameters required to characterize the behavior of any given soil can then be derived *entirely* from the results of conventional monotonic axial and cyclic strain-controlled simple shear soil tests [7-9]. As an illustration, Tables 1 and 2 give the parameter-values for the Cook's Bayou sand [7] and the Drammen clay [1]. These parameters were determined by using *solely* the results of axial compression/extension soil tests. Figs. 2 and 3 show the model predictions for both axial compression and consolidation/swelling tests, respectively, performed on the Cook's Bayou sand. Figs. 4 and 5 show the model predictions for both undrained axial and simple shear tests, respectively, performed on the Drammen clay (in Fig. 5 τ_h denotes the average horizontal shear stress measured experimentally). Fig. 6 shows the model predictions for cyclic stress- and strain-controlled simple shear and axial tests performed on the Drammen clay. Note that the model predictions agree very well with the experimental test results for all cases.

APPLICATION TO SOLUTION OF BOUNDARY VALUE PROBLEMS

Attention is restricted in the following to "quasi-static" loading conditions. The finite element formulation of the above governing equations (Eqs. 1-6) is performed by using the Galerkin procedure (see e.g. Ref. [14]). The class of constitutive equations assumed leads directly to the definition of tangent stiffness matrix. A simple backward difference scheme is adopted for the numerical time integration [11] in transient analysis. Further, in order to increase its accuracy, a predictor-corrector type algorithm is used at each time step (see Ref. [5] for further details). In the following sections, a number of examples are presented which demonstrate the versatility and accuracy of the proposed formulation in solving boundary value problems of interest in soil mechanics.

1. Two-Dimensional Elastoplastic Consolidation [11]

The finite element mesh and problem description are shown in Fig. 7a. A rigid permeable strip footing of width $2B$ is resting on the surface of a soil layer with drainage occurring at the top surface only. The mechanical properties of the soil to be considered in this example are shown in Figs. 2 and 3. The model parameter values (Table 1) have been normalized by dividing them by $\sigma_{vs}' =$ vertical effective consolidation stress. The soil deposit is assumed to be normally consolidated, and $\sigma_{vc}' = \gamma' z$ where z is the depth measured from the top surface of the deposit, and $\gamma' = (1-n^w)\rho_s$. In the following, $n^w = 0.7$, $\rho_s/\rho_w = 2.82$, and $k^{ws} = 2.10^{-6}$. The transient response of the soil deposit under the footing load is dependent upon the rate of loading w , $w = \frac{1}{\mu^s} \frac{dh}{dt}$ where $T = \bar{C}_v t/B^2$; $\bar{C}_v = 2\mu^s n^w k^{ws}/\rho_w$; and μ^s is selected to be the initial (at time $t=0$) shear modulus at depth $Z=B/2$, (i.e., $\mu^s = 120.0$). At very slow loading rates (i.e., $w \rightarrow 0$) the soil deposit's response is fully drained, whereas when the loading rate becomes large (i.e., $w \rightarrow \infty$), the deposit behaves in an undrained (i.e. constant volume) fashion. This is illustrated in Fig. 7b which shows the computed load/

settlement curves for various loading rates. These calculations were performed by neglecting changes in geometry (i.e. small strains/displacement), by including the effects of gravity, and by taking $\Delta t_n = 8 \Delta t_{n-1}$ with $\beta=1.1$, so that loading could be achieved in 16 steps only.

2. Wave-Offshore Structure-Soil Interaction [12]

In order to make the present study quite specific, attention herein is concentrated on the behavior of a fully saturated clay foundation for which the repeated loading resulting from wave forces during one individual storm is assumed to occur with no volume change. Furthermore, the foundation material is assumed to consist of a homogeneous deposit of Drammen clay (Figs. 4-6).

Due to the necessity of working within limited computation budgets, the problem geometry is transposed into 2-dimensions by assuming that it is of plane strain. Its 2-dimensional finite representation is shown in Fig. 8a. The structure foundation is represented by a strip footing which consists of a thin layer of elements a thousand times stiffer than the supporting soil. Fig. 8b shows the load system and notation. In addition to the static load W due to the dead weight of the structure, the foundation is also subjected to the cyclic inclined eccentric load F due to the wave forces, and Fig. 8c shows the time histories for its components V , H and M over a complete cycle of loading. For the purpose of illustration, $W/ACu = 3.42$ in the following, where $Cu = 0.584 \sigma'_{vc}$ denotes the static (unsoftened) undrained simple shear strength of the clay, and A the footing area. The computed load-displacement curves for the first 5 cycles of loading are shown in Fig. 8d, from which the progress of the various deformations can easily be traced: δ and d denote the vertical and horizontal displacements of the center of the foundation, respectively, and θ its tilt.

REFERENCES

- [1] Anderson, K.H. (1976), "Behavior of Clay Subjected to Undrained Cyclic Loading," Proceedings, BOSS 76 Conf., Trondheim, Norway, Vol. 1, pp. 392-403.
- [2] Biot, M.A. (1955), "Theory of Elasticity and Consolidation for a Porous Anisotropic Solid," J. Applied Physics, Vol. 26, pp. 182-185.
- [3] Forrest, J.H., et al. (1976), "Experimental Relationships Between Moduli for Soil Layers Beneath Concrete Pavements," Report No. FAA-RD-76-206.
- [4] Hill, R. (1958), "A General Theory of Uniqueness and Stability in Elastic-Plastic Solids," J. Mech. Phys. Solids, Vol. 6, pp. 236-249.
- [5] Hughes, T.J.R. and J.H. Prevost (1979), "DIRT II - A Nonlinear Quasi-Static Finite Element Analysis Program," California Institute of Technology, Pasadena, California.
- [6] Hvorslev, M.J. (1937), "Über die Festigkeitseigenschaften gestörter bindiger Boden," Ingeniørvidenskabelige Skrifter, A. no. 45, Copenhagen.

- [7] Prevost, J.H. (1977), "Mathematical Modeling of Monotonic and Cyclic Undrained Clay Behavior," Int. J. Num. Analyt. Methods in Geomechanics, Vol. 1, No. 2, pp. 195-216.
- [8] Prevost, J.H. (1978), "Anisotropic Undrained Stress-Strain Behavior of Clays," J. Geotech. Eng. Div., ASCE, Vol. 104, No. GT8, 1978, pp. 1075-1090.
- [9] Prevost, J.H. (1978), "Plasticity Theory for Soil Stress-Strain Behavior," J. Eng. Mech. Div., ASCE, Vol. 104, No. EMS, pp. 1177-1194.
- [10] Prevost, J.H. (1980), "Mechanics of Continuous Porous Media," Int. J. of Engineering Science (to appear).
- [11] Prevost, J.H. (1980), "Consolidation of Anelastic Porous Media," J. Eng. Mech. Div., ASCE (in process).
- [12] Prevost, J.H. Hughes, T.J.R and M.F. Cohen (1980), "Analysis of Gravity Offshore Structure Foundations," Journal of Petroleum Technology (to appear).
- [13] Terzaghi, K. (1943), Theoretical Soil Mechanics, Wiley, New York.
- [14] Zienkiewicz, O.C. (1977), The Finite Element Method, McGraw Hill.

TABLE 1: COOK'S BAYOU SAND $\sigma'_{vc} = 50$ psi - MODEL PARAMETERS

$$G_1 = 2000 \text{ psi}, \quad E_1 = 22320 \text{ psi}, \quad \alpha = 0.3, \quad \lambda = 148.1$$

n	σ_n (psi)	σ'_n (psi)	λ_n (psi)	E_n (psi)	G_n (psi)	α_n
2	24.00	60.24	32.36	27610.00	-6865.00	-0.1384
3	28.07	60.81	36.38	23870.00	-5724.00	-0.2380
4	32.16	61.39	40.23	20300.00	-5482.00	-0.3466
5	37.28	60.68	43.63	16830.00	-5041.00	-0.5810
6	41.54	61.67	46.23	13670.00	-4688.00	-0.7730
7	46.05	62.47	53.18	10860.00	-3873.00	-0.8836
8	51.68	61.86	64.61	8476.00	-2485.00	-1.020
9	62.95	66.29	77.47	5005.00	-1896.00	-0.9069
10	65.78	68.33	88.34	3599.00	-1478.00	-0.9391
11	66.31	74.75	105.80	2617.00	-1234.00	-0.8995
12	68.80	85.24	127.80	1811.00	-908.90	-0.8664
13	66.64	83.18	153.00	1379.00	-574.20	-1.062
14	67.23	109.30	196.30	619.70	-286.60	-1.008
15	122.68	121.50	261.50	0.00	0.00	-1.133

TABLE 2: BRANIFF CLAY $\sigma'_{vc} = 5$ - MODEL PARAMETERS

$$G_1 = 200 \sigma'_{vc}$$

n	σ_n (psi)	σ'_n (psi)	λ_n (psi)	E_n (psi)	G_n (psi)	α_n
2	0.100	0.300	266.867			
3	0.150	0.350	131.315			
4	0.300	0.400	100.000			
5	0.400	0.700	75.333			
6	0.415	0.775	54.667			
7	0.525	0.875	49.000			
8	0.530	0.950	31.000			
9	0.575	1.025	24.333			
10	0.680	1.050	17.333			
11	0.175	1.125	13.333			
12	0.880	1.200	10.000			
13	0.830	1.230	6.667			
14	0.825	1.275	5.333			
15	0.867	1.375	0.000			

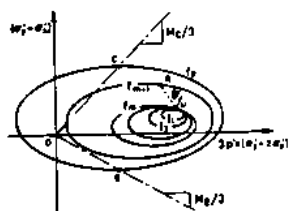


Fig. 1:
Field of Yield Surfaces

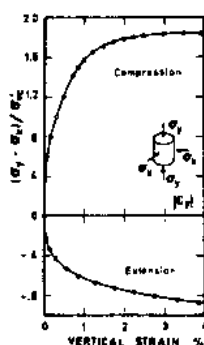


Fig. 4:
Drammen Clay: Axial Tests

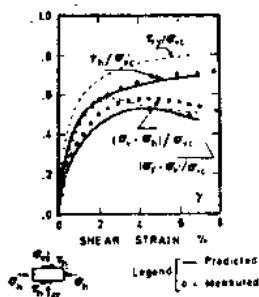


Fig. 5:
Drammen Clay:
Simple Shear Tests

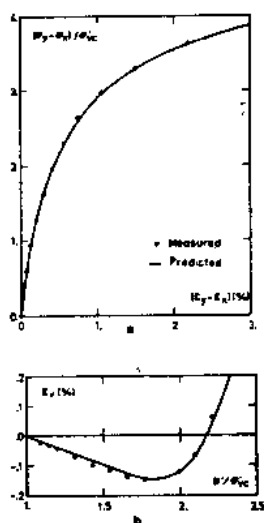


Fig. 2: Cook's Bayou Sand:
Axial Compression Tests

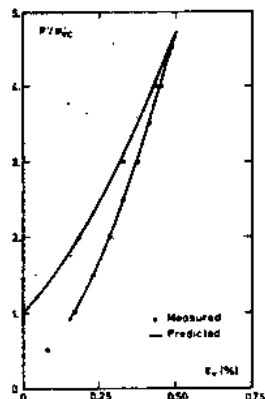


Fig. 3
Cook's Bayou Sand:
Consolidation/
Swelling Tests

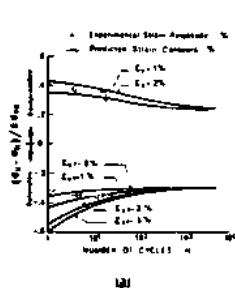
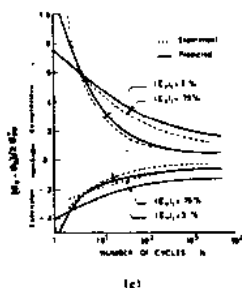
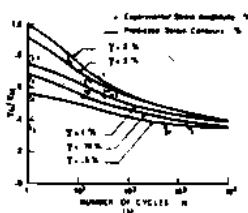
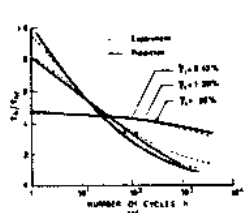


Fig. 6:
Drammen Clay, Cyclic Tests:

- Simple Shear Axial
- (a) Strain-controlled (a) Strain-controlled
- (b) Stress-controlled (b) Stress-controlled

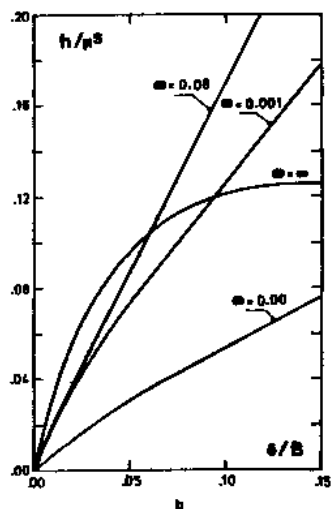
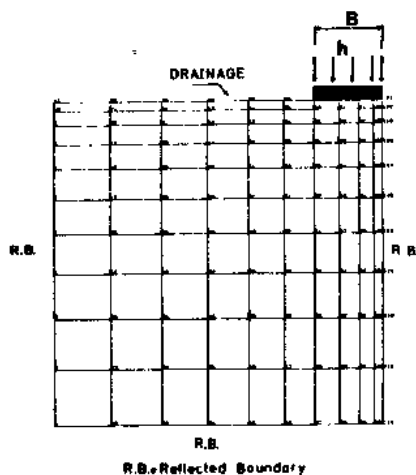


Fig. 7:

Anelastic Consolidation

(a) Finite Element Mesh

(b) Load Displacement

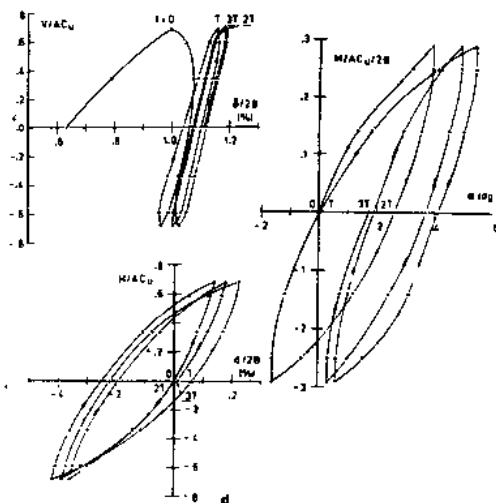
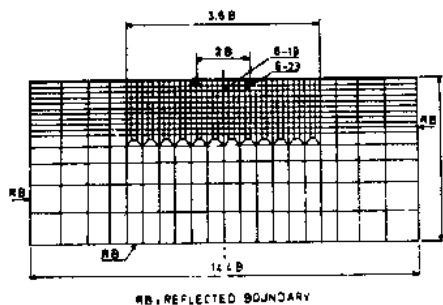


Fig. 8

Wave-Offshore Structure-Soil Interaction:

(a) Finite Element Mesh

(d) Computed Displacements

(b) Loading Conditions

(c) Wave Load Functions

A FINITE DIFFERENCE MODEL FOR LIQUEFACTION ANALYSIS

by

Atilla M. Ansal¹, Ali A. Elzaroughi², Raymond J. Krizek³ and Zdenek P. Bazant³

ABSTRACT

The response of a saturated sand deposit to earthquake motions is dominated by a progressive increase in pore pressure caused by the continuous rearrangement of the sand grains during each cycle of loading. This increase in pore pressure causes a reduction in the shear strength of the sand and, under certain conditions, may lead to liquefaction. The analysis of this phenomenon requires (a) a realistic constitutive law to model the inelastic nonlinear behavior of the sand, (b) a realistic theory to determine the pore pressure response for undrained conditions, and (c) a suitable mathematical scheme to evaluate the field situation. In the proposed model all three aspects were taken into account by use of an endochronic constitutive relationship and a two-phase medium concept to describe the pore pressure behavior. A one-dimensional finite difference scheme is formulated to model shear wave propagation for the soil conditions that prevail in Niigata, Japan, where liquefaction was observed during the 1964 earthquake. Using the same soil and site conditions, the governing equations for the propagation of compression waves are developed and the effects of vertical excitations is investigated for free and mass boundary conditions on the surface of the sand deposit.

INTRODUCTION

Virtually all studies performed during the last decade or two to investigate the liquefaction of sands have resulted in analytical procedures which are largely empirical in nature and based primarily on laboratory observations. Although some of the analytical methods that have been developed are based on constitutive laws, even these models do not adequately describe the nonlinear inelastic behavior of saturated sands under cyclic loading. The purpose of this study is to evaluate the capabilities of a new liquefaction model based on an endochronic constitutive law. The mathematical approach originated in the theory of viscoplasticity, and the inelastic response is described in terms of a state variable called intrinsic time. This variable is defined semi-empirically by taking microstructural changes into consideration in a macroscopic way. The two-phase medium concept (Biot, 1956) is incorporated into the formulation to account for the pore pressure behavior; in this approach a saturated sand element is assumed to consist of two interacting portions of continuum materials, a solid phase (grain structure) and a fluid phase (pore water). The model is capable of accounting for the hysteretic nonlinear shear behavior, as well as densification and pore pressure response, of a saturated sand subjected to cyclic loading. A one-dimensional finite difference scheme based on shear wave propagation is developed to evaluate the susceptibility of sand deposits to liquefaction. The model is then applied to the site conditions in Niigata, Japan, where liquefaction was observed during the 1964 earthquake. The effect of vertical excitations on the behavior of sand is investigated for two different boundary conditions, an unloaded boundary and one where a distributed load is applied to the surface.

-
1. Assistant Professor of Geotechnical Engineering, Macka Civil Engineering Faculty, Istanbul Technical University, Istanbul Turkey
 2. Assistant Professor of Geotechnical Engineering, Al-Fatih University, Tripoli, Libya
 3. Professor of Civil Engineering, Northwestern University, Evanston, Illinois, USA

CONSTITUTIVE MODEL

Endochronic constitutive relationships have been used successfully to model the stress-strain behavior of concrete (Bazant and Bhat, 1976), dry sand (Cuellar et al, 1977), and clays (Ansari, Bazant, and Krizek, 1979). The formulation used in this investigation is similar to that proposed by Cuellar et al (1977) and Elzaroughi et al (1979). Based on the assumption of isotropy, the stress-strain relations for a single phase medium can be expressed in terms of deviatoric and volumetric components as

$$de_{ij} = \frac{ds_{ij}}{2G} + \frac{S_{ij}}{2G} dZ \quad (1)$$

$$de_{kk} = \frac{d\sigma_{kk}}{3K} + 3d\lambda \quad (2)$$

where e_{kk} is the volumetric strain, σ_{kk} is the volumetric stress, $e_{ij} = e_{ij} - \delta_{ij}e_{kk}$ is the deviatoric strain, $S_{ij} = \sigma_{ij} - \delta_{ij}\sigma_{kk}$ is the deviatoric stress, G and K are the shear and bulk moduli of the soil structure, respectively, Z is an intrinsic time parameter that accounts for the inelastic response in the deviatoric stress-strain behavior, and λ is a parameter that represents the inelastic volumetric strain. Assuming that inelastic strains develop gradually from the very beginning of the stress path, the intrinsic time increment, dZ , can be written as

$$dZ = d\zeta/Z_1 \quad (3)$$

$$d\zeta = d\eta/f(\eta) \quad (4)$$

$$d\eta = F(e, \sigma) d\xi \quad (5)$$

$$d\xi = \sqrt{J_2(d\epsilon)} \quad (6)$$

The variable ζ , called the rearrangement measure, reflects the effects of the accumulated rearrangement of grain configurations on a macroscopic scale; analytically it is composed of a strain softening function, $F(e, \sigma)$, and a strain hardening function, $f(\eta)$. The variable ξ , called the distortion measure, depends only on the deviatoric strain, as shown by Bazant and Bhat (1976), where $J_2(d\epsilon)$ is the second invariant of the deviatoric strain increment. The increment of inelastic volumetric strain, $d\lambda$, is defined (Cuellar et al, 1977) as

$$d\lambda = dK/C(K) \quad (7)$$

$$dK = C(e, \sigma) d\xi \quad (8)$$

where K is the densification measure and $C(K)$ is the densification-hardening function. Since the inelastic volumetric strain defined in Equation (7) is assumed to be due only to shear strains, the densification measure increment, dK , is dependent on the distortion measure increment, $d\xi$.

Although the constitutive relations given in Equations (3), (4), (5), (7), and (8) were developed by Cuellar et al (1977) based on data from strain-controlled cyclic simple shear tests on dry sand, Elzaroughi et al (1979) have shown that this model with few modifications also yields realistic results for the cyclic behavior of saturated sands. In dealing with saturated sands, however, it appears more logical to treat the soil as a two-phase medium composed of water and a solid skeleton; in this way the interaction between the two phases can be taken into account through the volumetric inelastic strain relation by introducing a coupling parameter to link the separate behaviors of the solid skeleton and the pore fluid. Elzaroughi et al (1979) showed that the two-phase medium formulation suggested by Bazant and Krizek (1975) leads to a realistic model when used in conjunction with endochronic stress-strain relations.